Synthetic experiments to investigate occupant variability in braking manoeuvres, a simulation study using Active Human Body Models

Emma Larsson, Johan Iraeus, Johan Davidsson

Abstract During evasive manoeuvring, substantial variability is seen in volunteer displacements, with standard deviations typically at 50% of average displacements. Volunteer characteristics such as sex, stature, age and BMI explain some of the variation. In an attempt to identify other sources of the variation, this study replicated a physical experiment with passengers in braking, using Active Human Body Model simulations, by modeling a synthetic experiment to quantify the expected variation in kinematics, to identify the parameters accounting for most of this variation, and to quantify the expected influence on displacements of these parameters. First, a sensitivity study of boundary conditions was conducted to determine which boundary condition parameters were most important to explain the volunteer response variability. Secondly, the synthetic experiments were conducted by randomly sampling influential boundary condition parameters together with influential human characteristics. The parameters, sampled using Latin Hypercube, were seat longitudinal position, vehicle velocity change, belt stiffness, occupant posture and muscle strength. Results indicate that the most important sources of variability among the investigated parameters were seat position and occupant posture, which explain 70–80% of variation in peak displacements and 60% of variation in timing of peak seen in simulations. Together, the six investigated parameters captured 25–30% of variation of forward displacements seen in the physical experiments.

Keywords Active human body model, kinematics, pre-crash braking, sensitivity analysis, variability.

I. INTRODUCTION

Many newer vehicles are equipped with crash-avoidance systems, such as automated emergency braking [1]. While these systems are expected to prevent many crashes [2-5], if an accident is not avoided the manoeuvre could influence the injury outcome, by changing the occupant position and muscle activation [6-15].

Human body models (HBMs) are used to predict occupant response in crashes and in evasive steering and braking. There are several HBMs available that model the occupant response in these pre-crash events, utilising feedback control to emulate muscle reflexes. These models have all been validated using volunteer experiments [16-22].

Several studies have reported occupant kinematics in evasive steering and braking or low-speed frontal impacts from volunteer experiments [6-8][23-27]. Common to all of the studies was the large variability observed, with typical standard deviations of around 50% of average displacements. In some of the studies, efforts were made to attribute some of this variability to occupant characteristics, such as sex, stature, age or BMI. Some of the variability can be explained by these characteristics, but not all. Since the occupants have the ability to influence their kinematics in these low-loading scenarios [7][24][28], one hypothesis is that it could be the voluntary action that induces the variability [25][27]. Another is that it could come from other occupant characteristics that have not yet been investigated, such as body shape, degeneration, muscle strength or posture [21][27][29].

Recent efforts have been made, using volunteer experiments and simulations, to attribute these variations to parameters unrelated to sex, stature, age, BMI, or voluntary action. The initial posture was found influential of posture stabilisation in vibrational tests with volunteers [30]. In a large volunteer test series, among other effects, seat position forward-rearward position was found to be influence forward displacements in braking [25]. In another study, head posture was found to influence neck muscle activation in braking tests [31], and in yet

E. Larsson is a PhD student, J. Iraeus is a Researcher and J. Davidsson (e-mail: johan.davidsson@chalmers.se, Phone +46730346436) is an Associate Professor at the Division of Vehicle Safety, Chalmers University of Technology, Gothenburg, Sweden.

another study occupant position and posture were found to influence influential peak forward displacements in braking simulations [32]. This aligns with another study, where posture and muscle strength were found to influence kinematics in simulations of braking manoeuvres [29].

While these simulation studies investigated kinematic variability based on variability in model parameters, none of them quantified how much variability would be expected when varying these parameters according to a distribution expected for the population of occupants. Thus, the aim of this study was to replicate a physical experimental series, with volunteers exposed to braking, using simulations of a synthetic experiment to identify the parameters accounting for most of the variation in kinematics, and to quantify the expected variation in kinematics attributed to the parameter variations.

II. METHODS

The study was conducted in two steps. First, a sensitivity analysis of kinematic response to boundary condition variations was conducted, as a complement to a previous study where characteristics of the HBM were varied [29]. Secondly, with the most important boundary condition parameters identified, a synthetic experimental series was conducted by random sampling of the three most important boundary conditions and the three most important HBM characteristics: spinal alignment (defined using two parameters) and muscle physical cross-sectional area (PCSA).

SAFER HBM v10 [33] was used in this study, with the elements representing erector spinae longissimus thoracis and erector spinae iliocostalis lumborum rerouted according to [29], and the neck muscle controller gains updated according to [34]. All simulations were performed with LS-DYNA MPP R12.1.0 Double Precision (revision R12.1-190-gadfcdf9018, LST, Livermore, CA, USA). Pre-processing was done in ANSA v22.1 (BETA CAE Systems, Switzerland) and MATLAB R2022a (The Mathworks Inc., Natick, MA, US). Post-processing was performed using MATLAB R2022a and META v22 (BETA CAE Systems, Switzerland).

Physical experiments

The reference data in the current study came from an in-vehicle test series, where volunteers in the front-row passenger seat were exposed to different vehicle manoeuvres with lateral and longitudinal acceleration components [9][27][35-36]. The tests were performed with a Volvo V60, equipped with robot steering, an unmodified leather seat in the lowest position, the fore aft seat position adjusted to encompass proper foot support, and a 3-point seatbelt. The volunteers were asked to sit normally, with their hands in their lap, and look straight ahead. Head and torso translational and rotational displacements, belt forces and belt position for the front seat passengers were presented with regression models, using sex, stature, age, BMI and seatbelt characteristics as co-variates [27].

In the current study, corridors for a 45-year-old male with a stature of 175 cm and a BMI of 25 kg/m2, corresponding to the SAFER HBM, in braking manoeuvres with a standard seatbelt (i.e. belt pre-pretensioner turned off) were used for all kinematic comparisons. Additionally, the individual seatbelt force, position measurements and acceleration recordings were made available and used to vary boundary condition parameters (although not directly available from [27]). To allow for comparison between volunteer experiments and synthetic experiments, average and standard deviation (SD) of peak forward displacement and time to peak forward displacement (TTP) for head and torso were calculated from all individual displacements (from the displacement before regression models were created, again not directly available from [27]). All kinematic results are presented in a vehicle coordinate system with the x axis in the forward direction and positive z in the downward direction.

Simulation setup

In all simulations, a model of the seat and seatbelt from a Volvo V60 (and XC60) (Fig. 1) was used [18-19][29][37-38]. Acceleration in longitudinal direction was applied at the vehicle centre of gravity, while accelerations in the other directions were omitted. The retractor was modeled using a LS-DYNA seatbelt retractor. The portion of the belt running over the occupant was modeled using 2D seatbelt elements. The remaining parts, including the portion of the belt running through the D-ring and through the buckle, were modeled using 1D seatbelt elements. In all simulations the model was positioned as close as possible to the seat cushion and the seatback without introducing penetrations. The model was then gravity settled during 500 ms. The reference positions for the muscle controllers (neck and lumbar) were determined at 250 ms. The retractor element was locked at 350 ms, i.e. during gravity settling, prior to loading onset. The belt lock from experiments was modeled using a bi-linear

force-pull out curve in the retractor element, with a stiffer range after locking, which occurred at a specified pull-out and force, based on the experimental data. Belt slack during gravity settling was removed by specifying a 6 N belt pre-load in the retractor. The arms were constrained to the thighs using constant force cables, with a force of 10 N per arm. HBM-to-seat contact friction coefficients (static and dynamic) were set to 0.3. The footrest was positioned as close to the feet as possible without introducing penetrations.

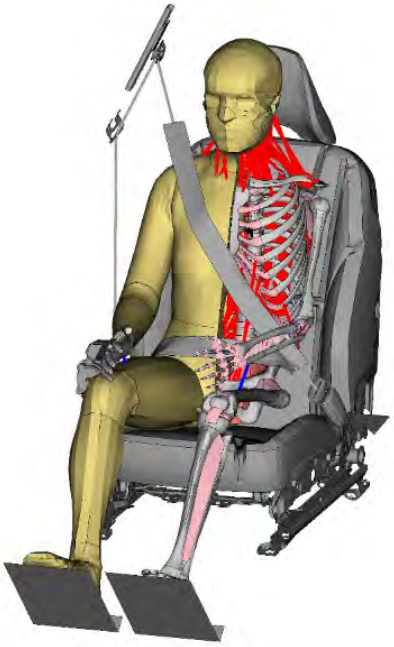

Fig. 1. SAFER HBM positioned in the seat. Pretensioned cables between arms and thighs in blue and active muscles in red. Internal organs, passive muscles and left-hand side skin and flesh removed for visualisation.

TABLE I
SUMMARY OF REFERENCES AND ASSUMED DISTRIBUTIONS FOR ALL PARAMETER VARIATIONS

Parameter	References	Distribution
Retractor film spool slope	[27]	Normal
Retractor film spool lock	[27]	Normal
Vehicle acceleration shape	[27]	Normal
Vehicle change in velocity	[27]	Normal
Seat position	Estimated from seat travel [27]	Uniform
D-ring (vertical) position	Estimated from volunteer seated heights [27]	Uniform
Friction coefficient	Estimated based on [39]	Uniform
Arm constraint	Estimated, artificial constraint	Uniform

Step 1 - Boundary condition sensitivity

The sensitivity of displacements to the boundary conditions used in simulations of braking (Table I) was investigated using the multiplicative dimensional reduction method (M-DRM) [40]. In short, the variance of the model's response to parameter variation is approximated through one-at-the-time parameter variation and computed using one-dimensional integrals using Gaussian quadrature. With the M-DRM, a model with n parameter variations and N Gauss points requires at most nN simulations to approximate the variance. If the nominal model is the same for all parameters, n(N-1) + 1 simulations are required. In this part of the study, three Gauss points were used in the evaluation. Eight parameters were varied, giving a total of 17 simulations. Additional information on M-DRM can be found in Appendix I.

Parameter variations

Most of the parameter distributions were based on distributions from the volunteer experiments (Table I). Appendix II describes the process of obtaining the parameter distributions. Resulting peak forward head and torso kinematics and time to peak (TTP) were used to evaluate the sensitivity. If all parameters had equal contribution, the sensitivity for each parameter would have been 1/8, and thus this value was used to evaluate if a parameter was influential or not. A sensitivity above 1/8 indicates a relatively important parameter, and lower sensitivity indicates a parameter of less importance.

Step 2 - Synthetic experimental series

After the most important boundary conditions were identified, Latin Hypercube sampling was performed to generate 20 simulation models. The three most important HBM parameters (Spinal alignment PC 1, Spinal alignment PC 2, and muscle PCSA) [29], and the three most important boundary condition parameters identified

in step 1, were included in the sampling. LS opt was used to generate the samples (see Table AI in Appendix III).

Parameter variations

The HBM parameters are described briefly in the sections below, and more details are found in [29].

Spinal alignment

The spinal alignments in [29] were based on segmental angles presented by [41-42]. In the [29] study, segmental angles were transformed to vertebral positions and PCA was performed to parameterise the variation in spine curvature. The first two PCs, together accounting for 95% of the variability (Fig. 2) were included in the [29] sensitivity study, and both were found influential. The first PC describes variation between more upright and more reclined occupants. The second PC describes how the spinal curvature varies, from straighter to more slouched.

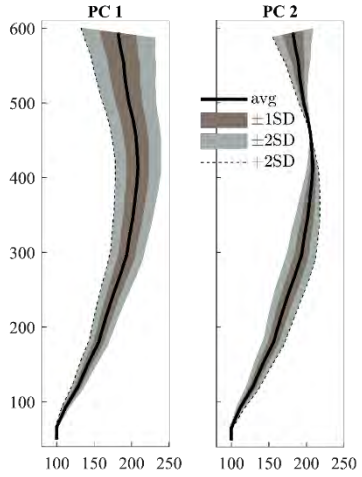

Fig. 2. Spinal alignment variations. The black line shows the average alignment, the filled brown area ±1SD, the filled grey area indicates ±2SD. PCs from [29], based on segmentation angles from [41-42]. The dashed black line shows +2SD.

Muscle strength

The muscle physical cross-sectional area (PCSA) was also found to influence the peak forward displacement [29]. In that study, an average coefficient of variation (defined as standard deviation divided by average) of 0.19, based on [43-46], was used to estimate the PCSA parameter variation. In the current study, nominal neck and lumbar muscle PCSA were scaled using the same coefficient of variation.

Simulation modifications

To modify the baseline HBM to the different spine postures, the HBM spine was aligned in a pre-simulation using the marionette method [47]. This was done for all the 20 sample points. After the pre-simulation, the nodal coordinates were extracted from the pre-simulation simulation results and transferred to the HBM model for the braking load case. Stresses and strains developed during the pre-crash simulation were not carried over. The HBMs with aligned spines were then positioned as close as possible to the seat without introducing penetrations between the seat and the HBM, and without rotating the HBM, as described in [29]. For two of the models, this resulted in a head-to-headrest initial penetration. This was solved by removing the contact between the HBM and headrest [29]. The belt was manually moved to remove any initial penetrations between the HBM and the belt. Belt slack was removed during gravity settling, as described in the *Simulation setup* section above.

To prevent neck extensors from becoming neck flexors with the straightened spine, some of the neck muscles were re-routed for this part of the study, see [29].

Comparing the synthetic population to the physical population

From the simulation results, head and torso translational kinematics averages and standard deviation corridors were calculated and overlayed on the volunteer corridors. Corridor widths were compared visually by overlaying the corridors, as well as by calculating the ratio between the corridor widths.

In order to analyse which of the six parameters accounts for most of the variability in the results, stepwise forward linear regression, with a maximum of two predictors (maximum 10 samples per predictor), was carried

out, in a similar way as in [48]. For each step in the forward stepwise selection, adjusted R2 was used to select the best model. To select the best among the models with one and two predictors, the p-value of the f-statistic (threshold, lower than 0.05) and adjusted R2 were used. To indicate the parameters "practical" effect, each regression coefficient was multiplied with the parameter range (±1 SD for normally distributed parameters, 66.6% of difference between lower and upper value for uniformly distributed parameters).

III. RESULTS

Step 1 - Boundary condition sensitivity

A general observed trend was that the model predicted the same as or slightly less forward displacement compared to the average volunteer (Fig. 3). Additionally, the model exhibited a rebound of head and torso after the first peak forward displacement, which was not seen in the volunteer kinematics. The two boundary parameters that changed the head and torso forward displacements most were seat position and the acceleration pulse velocity change. One of the vehicle acceleration shape variation parameters modulated the response curve to show an earlier head and torso x-displacement rebound, see Head and Torso x-displacements at about 1.7 s in Fig. 3, which is in line with the volunteer data. The parameter induced variations were symmetric for forward displacement, but asymmetric for lateral (y) displacement, where most of the variations led to smaller lateral displacement compared to the nominal model.

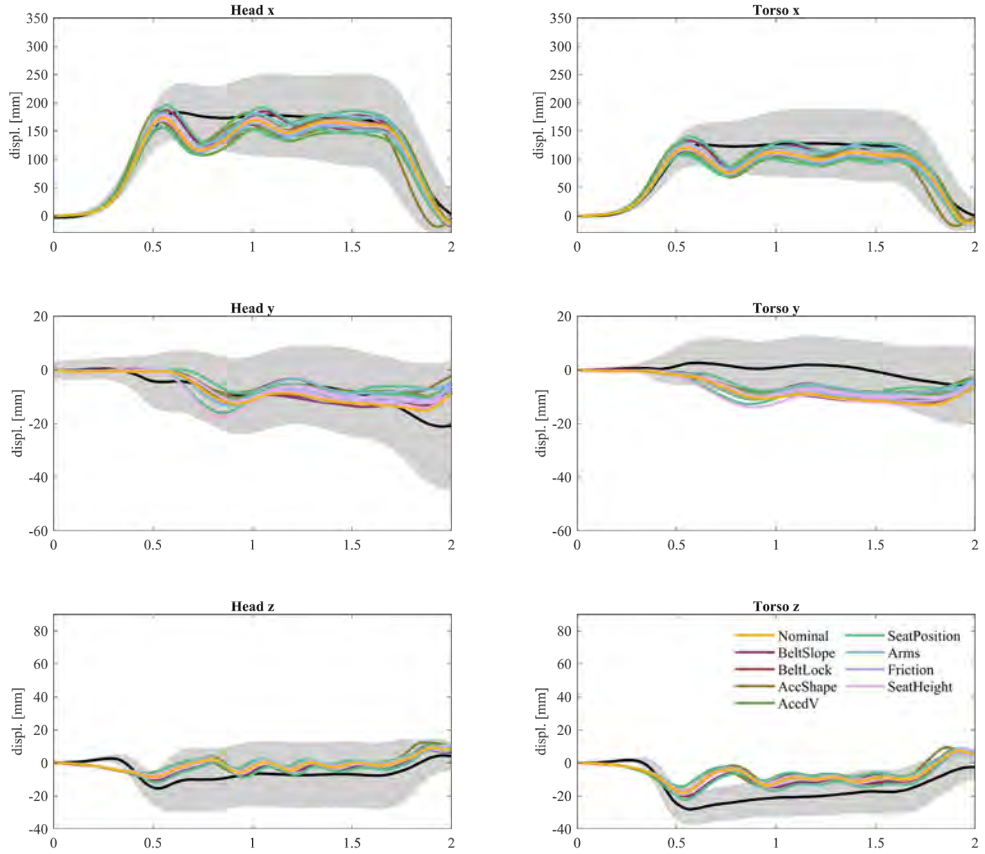

Fig. 3. Head and torso displacements, boundary condition sensitivity simulations compared to volunteer average (black) and corridors (grey).

The most influential boundary parameter, for all outputs, was the seat position parameter (Fig. 4). Also, vehicle velocity change (above average for all measurements), belt slope (higher than average for TTP) and vehicle acceleration shape (TTP) were important parameters to explain the variability in various kinematic responses. Finally, the friction, seat height, arm cable force, and belt lock had minimal influence on the kinematic results compared to the abovementioned parameters.

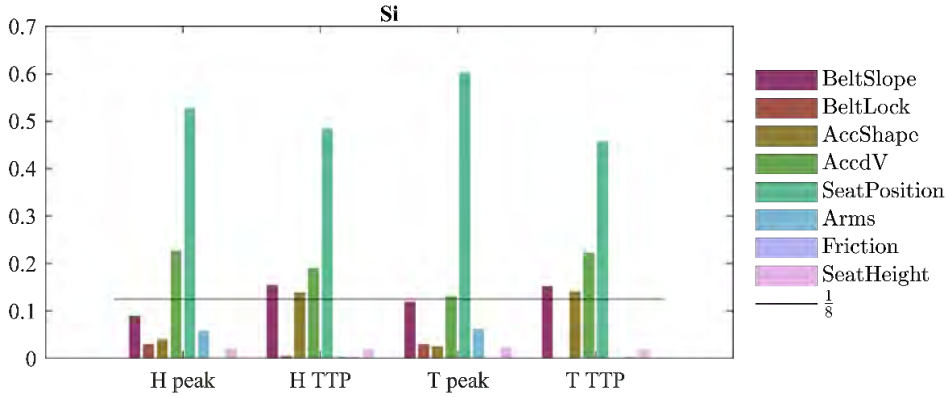

Fig. 4. Primary sensitivity index (peak and TTP) for head (H) and torso (T).

Step 2 - Synthetic experimental series

Generally, the predicted average head forward displacement was larger for the synthetic experiments, although with smaller variation, compared to the volunteer data (Fig. 5). The predicted torso forward displacement was similar in both magnitude and phase. Further, the predicted head and torso average lateral displacements, and the torso vertical displacement, were also in line with the volunteer responses. The major differences observed were the vertical head displacements, where the volunteers on average displaced slightly upwards, while the model on average predicted a slightly downwards displacement.

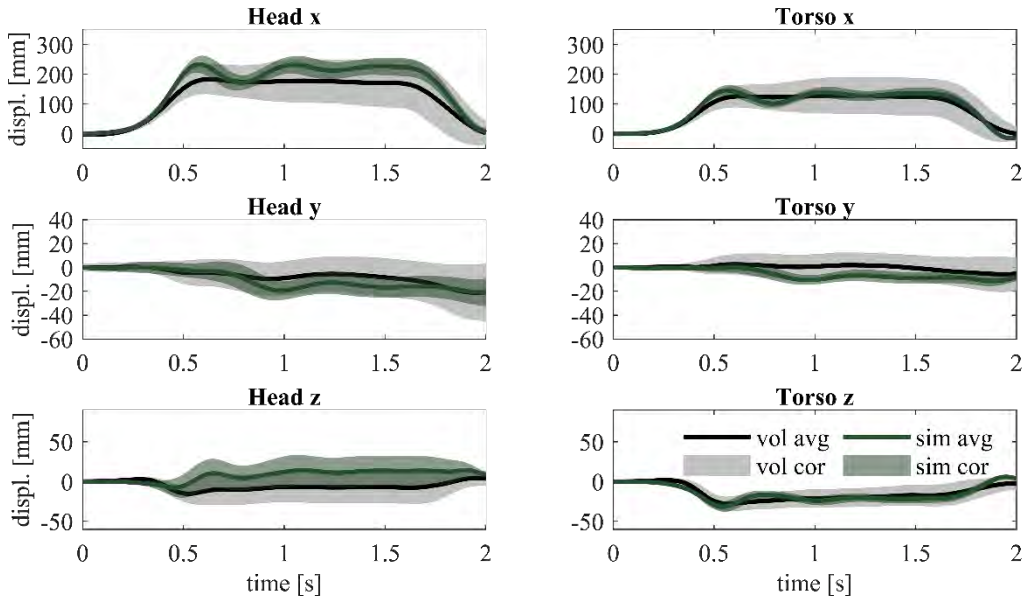

Fig. 5. Average displacements and corridors for physical experiments (black/gray), and synthetic experiments (green).

Comparing the corridor widths, the corridors created from simulations were narrower than the corridors from the volunteer tests, except for the head z displacement where the corridors were similar in shape and size (Fig. 6). Specifically, it was noticed that the simulation and the volunteer corridor widths were more similar early in the braking manoeuvre (0–0.7 s), compared to later in the manoeuvre, where the volunteer corridors widen while the simulation corridors remain at approximately the same width. Overall, the simulations captured around 25–50% of the variance in head x displacements, around 25% of the variance in torso x displacements, around 50% of the variance in y displacements, and 50–100% of the variance in z displacements, compared to the volunteer tests.

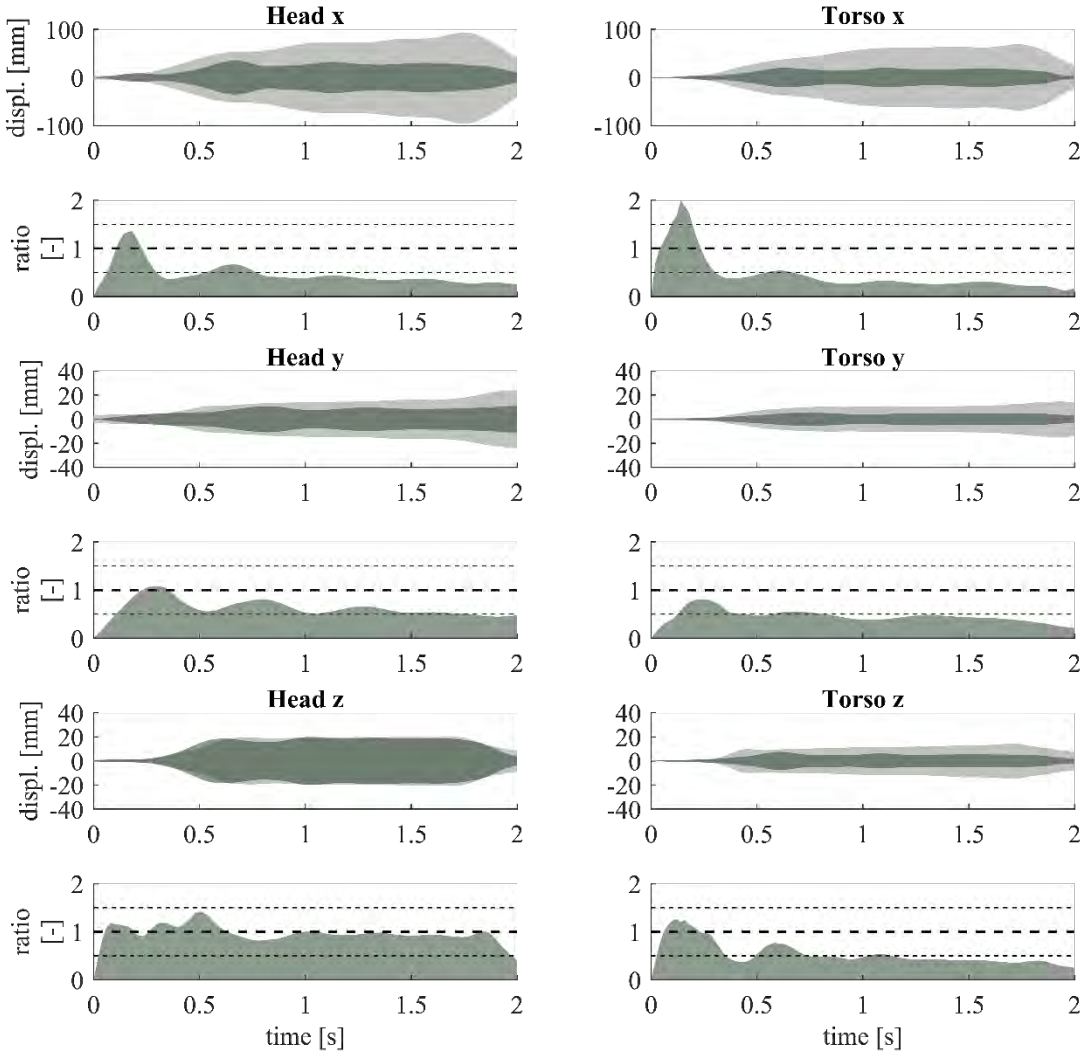

Fig. 6. Variance and variance ratio (width of simulation corridor divided by width of volunteer corridor) for head and torso displacements. Volunteer variance in grey, simulation variance in green. The thick dashed lines show equal variance, the thinner dashed lines indicate ratios of 0.5 and 1.5.

The regression models indicated that the most influential parameters, of all HBM and boundary condition parameters, were seat position and spinal alignment PC2 (Table II). A more forward position reduced the forward displacements and reduced the TTPs. For spinal alignment PC2, a more curved spine reduced the peak displacements and reduced TTPs. The parameters belt stiffness, muscle size, velocity change and spinal alignment PC1 were not among the two most influential parameters for any of the responses. In total, the two most influential parameters explained 70–80% of the variation in forward displacements and around 60% of the variation in TTP.

TABLE II
LINEAR REGRESSION RESULTS. EACH VALUE WAS MULTIPLIED BY THE SPECIFIED RANGE. FOR SEAT POSITION, THE RANGE INDICATED A SHIFT FROM A MORE REARWARD TO A MORE FORWARD POSITION. FOR SPINAL ALIGNMENT PC2, THE RANGE INDICATES A SHIFT FROM A STRAIGHTER TO A MORE CURVED SPINE

Parameter/measure	Head peak [mm]	Head TTP [ms]	Torso peak [mm]	Torso TTP [ms]
Seat position	-45	-23	-33	-23
Spinal alignment PC2	-28	-22	-14	-19
Adjusted R^2	0.70	0.59	0.79	0.58

IV. DISCUSSION

The aim of this study was to replicate a physical experimental series, with volunteers exposed to braking, using simulations of a synthetic experiment, and to quantify the expected variation in kinematics attributed to the parameter variations. The study utilised a novel method of combining physical experiments and simulations to advance the understanding of occupant variability. The main findings of this study were as follows.

- Of the investigated boundary condition parameters, the most influential was fore aft seat position, followed by belt stiffness and vehicle velocity reduction.
- In the synthetic experiments, the width of the forward displacement corridors was 25–50% of width from volunteer displacement forward corridors.
- In the synthetic experiments, the most influential parameters were seat position and spinal alignment PC2.
- Head vertical displacement corridors from the synthetic experiments were equally wide as the corridors from physical experiments.
- Corridors from synthetic experiments were more similar to the corridors from the physical experiments early in the manoeuvre compared to later in the manoeuvre.

The created corridors widths were 25–100% of corridor width from volunteer experiments. The synthetic vertical kinematic corridors were similar in width to the corridors from physical experiments, while the forward displacement corridors were narrower in the synthetic experiments compared to the physical experiments. As discussed in [29], this could indicate that the vertical kinematics is more related to physical characteristics, while the forward displacements might be more related to variations in control strategy selected by the occupants, or other characteristics not included in this analysis. Further, the corridors were more similar early in the manoeuvre compared to later in the manoeuvre (Fig. 6) when corridors for volunteers became wider while synthetic experiments corridor remained at the same width. The implemented controller emulates reflexes, which act on a short time scale, while voluntary action acts later [49-50]. Potentially, volitional control could explain why volunteer corridors widen while simulation corridors remain at a similar width throughout the manoeuvre. This suggests that the initial response from volunteers was dominated by a reflex response, similar for both repetitions and different volunteers. However, while further into the manoeuvre the volunteers adopted different voluntary strategies between the repetitions of the manoeuvre and between the different volunteers. In contrast, the model employed the same reflex-based control strategy for the entire duration, and for all repetitions.

When using both M-DRM and Latin Hypercube sampling methods, the distributions need to accurately represent the distribution within the studied population. For most of the parameters, the distributions were based on data from either the physical experiment or from literature. For other parameters, however, no information was available, or the parameters were artificial parameters (such as the arm cable force). For these parameters (seat position, D-ring position, friction, and arm cable force), uniform distributions were assumed, so as not to underestimate the parameter influence. While the model was relatively insensitive to most of these parameters, seat position was found influential, when assumed to be uniformly distributed from most forward to most rearward seat position. It is likely that the variation of seat position within the physical experiment was distributed differently, and thus it is possible that the effect from seat position was over-estimated in the M-DRM evaluation, and when comparing the corridor widths of the synthetic experiments to the physical experiments.

Head vertical displacement corridors from physical and synthetic experiments were equally wide. Although the variation in parameters were based on literature or variation in the physical experiment (except for seat position), it is unlikely that all variability in vertical displacement would be accounted for by these parameters in a physical experiment. Instead, one or more of the parameters was likely more influential than in the physical experiments. Since one of the spinal alignments was identified as influential in the head vertical displacements, and the cervical spines have previously been identified as straighter than in other populations [29], it is possible that the effect from spinal alignment was more influential in the synthetic experiments compared to the physical experiments.

In the boundary condition sensitivity analysis, the head x displacements were lower for simulation models than in the physical experiments (Fig. 3), while in the synthetic experiments the head displacements were larger than for the physical experiments (Fig. 5). The nominal model and average in Latin Hypercube simulations differ

only in spinal alignment. Most likely, the change in average spinal alignment from SAFER HBM original alignment to average from [41-42] caused this increase in head forward displacement. In [29], the average spinal alignment from [41-42] was discussed as potentially straighter than spinal alignments from other populations. Possibly, the average volunteer has a spinal alignment that is more curved than those used in the current study. According to the regression models (Table II), a more curved spine would reduce the forward displacements, and thus with a more curved spine the models would be more similar to the volunteers.

Just as for [25], seat position was found to influence the forward displacements in braking. In their study, a more forward seat position resulted in smaller forward displacements. The authors hypothesised that these reduced forward displacements could be due to a difference in seatbelt geometry. If not attributed to the belt geometry, it could be related to the volunteers restricting their movements due to the smaller head-interior distance. Since no volitional control was included in this study, the reduction in forward displacement was related to the belt geometry only. For the same difference in seat position (66% of 220 mm), using the regression models for peak displacement provided in [25], the peak displacement would be reduced by 48 mm, similar to the 45 mm in this study (Table II), indicating that the effect in their study was most likely more related to the belt geometry than to the voluntary head restriction.

Peak values and time to peak (TTP) varied more in the physical experiments than in the synthetic experiments. In the physical experiments, kinematics was sampled at 50 Hz, while the kinematics in the synthetic experiments was sampled at 1000 Hz. With the lower sampling frequency for volunteers, the accuracy of peak and TTP was lower than for the synthetic experiments. With 50 Hz sampling, the recorded and actual volunteer TTP could differ with up to 20 ms, while most likely within ±10 ms because displacement velocity just before and just after peak were relatively symmetric, and thus the peak would most likely be attributed to the frame closest in time to the true peak. Because the displacement velocity was relatively low just before and after the peak, the accuracy of peak value was within a few mm, with maximum movement between frames of around 6 mm, one frame before and one frame after peak. The SD of TTPs in physical experiments was around 70–80 ms, compared to around 20 ms for the synthetic experiments, which means that the difference from sampling frequency was not enough to explain the difference between variability of TTPs in physical and synthetic experiments.

Limitations and future work

A limited number of simulations could be performed within the study due to limited computer resources. If more simulations had been conducted, the effect from each of the six parameters could have been quantified, and important interactions as well. Instead, only the two most important parameters for each measure were identified using linear regression.

The M-DRM evaluations were performed with only three Gauss points. Typically, 5 Gauss points are used, thus there is a possibility that the results were not converged. Most likely this would affect ranking of parameters with similar importance. Since seat position was by far the most influential parameter, and velocity change second most influential, it is unlikely that the rank in importance for these parameters would have been changed with more Gauss points. With the same reasoning, the ranking for the least influential parameters (belt lock, friction, seat height) would also most likely not change. However, it is possible that the third most important parameter could have been acceleration shape or arm cables instead of belt stiffness.

In the second part of this study, the six most important parameters, as identified in [29] and in the first part of this study, were varied using Latin Hypercube sampling. Although the remaining parameters were omitted due to relative unimportance, including the remaining three parameters from [29] and the remaining parameters from the first part of this study, they would have most likely marginally increased the width of the corridors in this study.

These results can be used for several purposes. The results could be used when planning a volunteer braking experiment, or when setting up simulations of passengers in braking. The results in this study rank what should be carefully controlled (e.g. seat position and posture), or accounted for by regression models, and what is of less relevance (e.g. friction between model and seat). The results could also be used when trying to increase the knowledge on the relatively large variability between passengers in braking manoeuvres. If the results in this study are confirmed by a volunteer experiment, additional knowledge on what can be attributed to volitional control and what can be attributed to other characteristics can be gained. Additionally, the results could be used in the design of future seats and restraint systems, for instance by designing seats that promote a specific sitting

posture.

All simulations have been done with an inertia reel seatbelt only. Some modern vehicles use an electric reversible retractor to pre-pretension their seatbelts when automated accident-avoidance braking is initiated. Several studies have indicated that the relative importance of the standard seatbelt is high [6-7][27]. However, the results might not be representative of the occupant variability when another seatbelt system, such as an electric reversible seat belt system, is used.

V. CONCLUSION

The aim of the study was to replicate a physical experimental series, with volunteers exposed to braking, using simulations of a synthetic experiment to quantify the expected variation in kinematics attributed to the parameter variations. It was concluded that by varying the investigated parameters, 25–30% of variation of forward displacements seen in the physical experiments was captured. Results indicate that the most important sources of variability, among the investigated parameters, were seat position and occupant posture, explaining 70–80% of variation in peak displacements and 60% of variation in timing of peak seen in simulations. These results can be used when determining what data to collect from future volunteer experiments.

VI. ACKNOWLEDGEMENTS

The work was carried out within SAFER - Vehicle and Traffic Safety Centre at Chalmers, Gothenburg, Sweden and carried out by Chalmers University of Technology, Autoliv Research, Dynamore Nordic and Volvo Cars in the project Active human body models for virtual occupant response, step 5. The work was funded by FFI (Strategic Vehicle Research and Innovation), by VINNOVA, the Swedish Transport Administration, the Swedish Energy Agency, and the industrial partners. Simulations were performed on resources at NSC Tetralith provided by the Swedish National Infrastructure for Computing (SNIC), funded by the Swedish Research Council through grant agreement no. 2018-05973.

VII. REFERENCES

1. Highway Loss Data Institute HLDI (2022) Predicted availability of safety features on registered vehicles - a 2022 update. *Bulletin*, **39**(2): April 2022.
2. Östling, M., Lubbe, N., Jeppsson, H., Puthan, P. (2019) Passenger car safety beyond ADAS: Defining remaining accident configurations as future priorities. 26th International Technical Conference on the Enhanced Safety of Vehicles (ESV), 2019, Eindhoven, Netherlands.
3. Leledakis, A., Lindman, M., *et al*. (2021) A method for predicting crash configurations using counterfactual simulations and real-world data. *Accident Analysis & Prevention*, **150**: 105932.
4. Tan, H., Zhao, F., *et al*. (2020) Automatic emergency braking (AEB) system impact on fatality and injury reduction in China. *International Journal of Environmental Research and Public Health*, **17**: 917.
5. Seacrist, T., Sahani, R., *et al*. (2020) Efficacy of automatic emergency braking among risky drivers using counterfactual simulations from the SHRP 2 naturalistic driving study. *Safety Science*, **128**: 104746.
6. Ólafsdóttir, J. M., Östh, J. K. H., Davidsson, J., Brolin, K. B. (2013) Passenger kinematics and muscle responses in autonomous braking events with standard and reversible pre-tensioned restraints. *Proceedings of the IRCOBI Conference*, 2013, Gothenburg, Sweden.
7. Kirschbichler, S., Huber, P., *et al*. (2014) Factors influencing occupant kinematics during braking and lane change maneuvers in a passenger vehicle. *Proceedings of the IRCOBI Conference*, 2014 Berlin, Germany.
8. Holt, C., Seacrist, T., *et al.* (2020) The effect of vehicle countermeasures and age on human volunteer kinematics during evasive swerving events. *Traffic Injury Prevention*, **21**: pp. 48–54.
9. Ghaffari, G., Davidsson, J. (2021) Female kinematics and muscle responses in lane change and lane change with braking maneuvers. *Traffic Injury Prevention*, **22**: pp. 236–241.
10. Bose, D., Crandall, J. R., Untaroiu, C. D., Maslen, E. (2010) Influence of pre-collision occupant parameters on injury outcome in a frontal collision. *Accident Analysis & Prevention*, **42**: pp. 1398–1407.
11. McMurry, T. L., Poplin, G. S., Shaw, G., Panzer, M. B. (2018) Crash safety concerns for out-of-position occupant postures: A look toward safety in highly automated vehicles. *Traffic Injury Prevention*, **19**: pp. 582–587.
12. Nie, B., Sathyanarayan, D., Ye, X., Crandall, J. R., Panzer, M. B. (2018) Active muscle response contributes to increased injury risk of lower extremity in occupant–knee airbag interaction. *Traffic Injury Prevention*, **19**:

S76-S82.
13. Östh, J., Larsson, E., Jakobsson, L. (2022) Human Body Model Muscle Activation Influence on Crash Response. *Proceedings of the IRCOBI Conference*, 2022, Porto, Portugal.
14. Wass, J., Östh, J., Jakobsson, L. (2022) Active Human Body Model Simulations of Whole-Sequence Braking and Far-Side Side-Impact Configurations. *Proceedings of the IRCOBI Conference*, 2022, Porto, Portugal.
15. González-García, M., Weber, J., Peldschus, S. (2021) Potential effect of pre-activated muscles under a far-side lateral impact. *Traffic Injury Prevention*, pp. S148-S152.
16. Devane, K., Chan, H., Alabert, D., Kemper, A., Gayzik, F. S. (2022) Implementation and calibration of active small female and average male human body models using low-speed frontal sled tests. *Traffic Injury Prevention*, pp. 1–6.
17. Devane, K., Johnson, D., Gayzik, F. S. (2019) Validation of a simplified human body model in relaxed and braced conditions in low-speed frontal sled tests. *Traffic Injury Prevention*, pp. 1–6.
18. Larsson, E., Iraeus, J., *et al.* (2019) Active Human Body Model Predictions Compared to Volunteer Response in Experiments with Braking, Lane Change, and Combined Manoeuvres. *Proceedings of the IRCOBI Conference*, 2019, Florence, Italy.
19. Östh, J., Brolin, K., Bråse, D. (2015) A Human Body Model With Active Muscles for Simulation of Pretensioned Restraints in Autonomous Braking Interventions. *Traffic Injury Prevention*, **16**: pp. 304–313.
20. Martynenko, O. V., Neininger, F. T., Schmitt, S. (2019) Development of a Hybrid Muscle Controller for an Active Finite Element Human Body Model in LS-DYNA Capable of Occupant Kinematics Prediction in Frontal and Lateral Maneuvers. 26th International Technical Conference on the Enhanced Safety of Vehicles (ESV), 2019, Eindhoven, Netherlands.
21. Wochner, I., Nölle, L. V., Martynenko, O. V., Schmitt, S. (2022) 'Falling heads': investigating reflexive responses to head–neck perturbations. *Biomedical Engineering*, online, **21**: pp. 1–23.
22. Kato, D., Nakahira, Y., Atsumi, N., Iwamoto, M. (2018) Development of human-body model THUMS version 6 containing muscle controllers and application to injury analysis in frontal collision after brake deceleration. *Proceedings of the IRCOBI Conference*, 2018, Athens, Greece.
23. Van Rooij, L., Elrofai, H., Philippens, M., Daanen, H. (2013) Volunteer kinematics and reaction in lateral emergency maneuver tests. *Stapp Car Crash Journal*, **57**: p. 313.
24. Chan, H., Albert, D. L., Gayzik, F. S., Kemper, A. R. (2022) Occupant Kinematics of Braced 5th Percentile Female and 50th Percentile Male Volunteers in Low-Speed Frontal and Frontal-Oblique Sled Tests. *Proceedings of the IRCOBI Conference*, 2022, Porto, Portugal.
25. Reed, M. P., Ebert, S. M., Jones, M. H., Park, B.-K. D. (2021) Occupant Dynamics During Crash Avoidance Maneuvers. United States. Department of Transportation. National Highway Traffic Safety.
26. Reed, M. P., Ebert, S. M., *et al*. (2018) Passenger head kinematics in abrupt braking and lane change events. *Traffic Injury Prevention*, **19**: pp. S70–S77.
27. Larsson, E., Ghaffari, G., Iraeus, J., Davidsson, J. (2022) Passenger Kinematics Variance in Different Vehicle Manoeuvres – Biomechanical Response Corridors Based on Principal Component Analysis. *Proceedings of the IRCOBI Conference*, 2022 Porto, Portugal.
28. Carlsson, S., Davidsson, J. (2011) Volunteer occupant kinematics during driver initiated and autonomous braking when driving in real traffic environments. *Proceedings of the IRCOBI Conference*, 2011, Krakow, Poland.
29. Larsson, E., Iraeus, J., Davidsson, J. (2023) Investigating sources for variability in volunteer kinematics in a braking maneuver, a sensitivity analysis with an active Human Body Model. *Frontiers in Bioengineering and Biotechnology*, **11**:1203959.
30. Mirakhorlo, M., Kluft, N., Shyrokau, B., Happee, R. (2022) Effects of seat back height and posture on 3D vibration transmission to pelvis, trunk and head. arXiv preprint arXiv:2207.01989.
31. Kempter, F., Lantella, L., Stutzig, N., Fehr, J., Siebert, T. (2022) Role of rotated head postures on volunteer kinematics and muscle activity in braking scenarios performed on a driving simulator. *Annals of Biomedical Engineering*, pp. 1–12.
32. Erlinger, N., Kofler, D., Heider, E., Klug, C. (2022) Effects of Boundary Conditions and Posture on Simulations with Human Body Models of Braking Events. *Proceedings of the IRCOBI Conference*, 2022 Porto, Portugal.
33. Pipkorn, B., Östh, J., *et al.* (2021) Validation of the SAFER Human Body Model Kinematics in Far-Side Impacts.

Proceedings of the IRCOBI Conference, 2021, Online.
34. Larsson, E., Iraeus, J., *et al*. (2023) Predicting occupant head rotations; a new omni-directional neck muscle controller for active human body models. *Frontiers in Bioengineering and Biotechnology*, https://doi.org/10.3389/fbioe.2023.1313543.
35. Ghaffari, G., Brolin, K., *et al*. (2018) Passenger kinematics in Lane change and Lane change with Braking Manoeuvres using two belt configurations: Standard and reversible pre-pretensioner. *Proceedings of the IRCOBI Conference*, 2018, Athens, Greece.
36. Ghaffari, G., Brolin, K., Pipkorn, B., Jakobsson, L., Davidsson, J. (2019) Passenger muscle responses in lane change and lane change with braking maneuvers using two belt configurations: Standard and reversible pre-pretensioner. *Traffic Injury Prevention*, **20**: pp. S43–S51.
37. Östh, J., Brolin, K., Carlsson, S., Wismans, J., Davidsson, J. (2012) The Occupant Response to Autonomous Braking: A Modeling Approach That Accounts for Active Musculature. *Traffic Injury Prevention*, **13**: pp. 265–277.
38. Östh, J., Eliasson, E., Happee, R., Brolin, K. (2014) A method to model anticipatory postural control in driver braking events. *Gait & Posture*, **40**: pp. 664–669.
39. Valdano, M., Jiménez Octavio, J. R., Vives Torres, C. M., López Valdés, F. J., Pipkorn, B. (2021) Assessment of madymo active human body model kinematics and dynamics by means of human volunteer response at low-speed frontal impacts. *Proceedings of the IRCOBI Conference*, 2021, Online.
40. Zhang, X., Pandey, M. D. (2014) An effective approximation for variance-based global sensitivity analysis. *Reliability Engineering & System Safety*, **121**: pp. 164–174.
41. Izumiyama, T., Nishida, N., *et al*. (2018) The analysis of an individual difference in human skeletal alignment in seated posture and occupant behavior using HBMs. *Proceedings of the IRCOBI Conference*, 2018, Athens, Greece.
42. Nishida, N., Izumiyama, T., *et al*. (2020) Changes in the global spine alignment in the sitting position in an automobile. *The Spine Journal*, **20**: pp. 614–620.
43. Frantz Pressler, J., Givens Heiss, D., Buford, J. A., Childley, J. V. (2006) Between-day repeatability and symmetry of multifidus cross-sectional area measured using ultrasound imaging. *Journal of Orthopaedic & Sports Physical Therapy*, **36**: pp. 10–18.
44. Fortin, M., Gibbons, L., Videman, T., Battie, M. (2015) Do variations in paraspinal muscle morphology and composition predict low back pain in men? *Scandinavian Journal of Medicine & science in Sports*, **25**: pp. 880–887.
45. Kamaz, M., Kiresi, D., Ogusz, H., Emlik, D., Levendoglu, F. (2007) CT measurement of trunk muscle areas in patients with chronic low back pain. *Diagnostic and Interventional Radiology*, **13**: p. 144.
46. Savage, R., Mellerchip, R., Whitehouse, G., Edwards, R. (1991) Lumbar muscularity and its relationship with age, occupation and low back pain. *European Journal of Applied Physiology and Occupational Physiology*, **63**: pp. 265–268.
47. Poulard, D., Subit, D., Donlon, J.-P., Kent, R. W. (2015) Development of a computational framework to adjust the pre-impact spine posture of a whole-body model based on cadaver tests data, *Journal of Biomechanics*, **48**(4): pp. 636-643.
48. Iraeus, J., Brolin, K., Pipkorn, B. (2020) Generic finite element models of human ribs, developed and validated for stiffness and strain prediction–To be used in rib fracture risk evaluation for the human population in vehicle crashes. *Journal of the Mechanical Behavior of Biomedical Materials*, **106**: 103742.
49. Kurtzer, I. L. (2015) Long-latency reflexes account for limb biomechanics through several supraspinal pathways. *Frontiers in Integrative Neuroscience*, **8**: p. 99.
50. MacEfield, V. G. (2009) Long Loop Reflexes. In: Binder, M. D., Hirokawa, N. & Windhorst, U. (eds.), Encyclopedia of Neuroscience. *Springer Berlin Heidelberg*, Berlin, Heidelberg, Germany.
51. Eriksson, L., Byrne, T., Johansson, E., Trygg, J., Vikström, C. (2013) PCA. Multi-and megavariate data analysis basic principles and applications. Umetrics Academy.
52. James, G., Witten, D., Hastie, T., Tibshirani, R. (2021) Unsupervised Learning. An introduction to statistical learning. 2nd ed., *Springer*.
53. Jollife, I. T., Cadima, J. (2016) Principal component analysis: a review and recent developments. *Philosophical Transactions of the Royal Society A: Mathematical, Physical and Engineering Sciences*, **374**: 20150202.

VIII. APPENDIX

Appendix I - Multiplicative dimensional reduction method

In the multiplicative dimensional reduction method (M-DRM) [40], the output Y of a model depends on the input parameters $\mathbf{X} = [X_1, \dots, X_n]^T$, and can be described by a function $h(\mathbf{X})$. The function $h(\mathbf{X})$ is approximated with reference to a fixed input point with coordinates $\mathbf{c}$ (Equation 1). The function is approximated for one parameter at a time, while the other parameters are unchanged.

$$Y = h(\mathbf{x}) \approx h_0^{1-n} \prod_{i=1}^{n} h(x_i, \mathbf{c}_{-i}) \quad \text{(Eq. 1)}$$

The mean and mean square (ρ_i and θ_i) are then approximated using one-dimensional integrals, computed numerically with Gaussian quadrature (Equation 2). w_{ij} describes the Gauss weight for the ith parameter and j:th Gauss point.

$$\begin{cases} \rho_i \approx \sum_{j=1}^{N} w_{ij} h(X_i^j, \mathbf{C}_{-i}) \\ \theta_i \approx \sum_{j=1}^{N} w_{ij} \left[h(X_i^j, \mathbf{C}_{-i}) \right]^2 \end{cases} \quad \text{(Eq. 2)}$$

Using the approximative mean and mean square (ρ_i and θ_i), the primary sensitivity of the model to the selected parameter can be approximated according to Equation 3:

$$S_i \approx \frac{\theta_i / \rho_i^2 - 1}{\left(\prod_{k=1}^{n} \theta_k / \rho_k^2 \right) - 1} \quad \text{(Eq. 3)}$$

Appendix II - Parameter variations in the Boundary condition sensitivity study

Retractor spool out characteristics

To change the seatbelt parameters, the loading curve of the seatbelt retractor was parameterised. The loading curve characteristics were based on belt forces and belt positions from the volunteer experiments. For each volunteer test, the belt position (parameter one) and force (average used, never varied) when locking was identified by differentiating the force time series curve, and first occasion above a set derivative threshold was determined as locking. The off-loading was identified as the first instance, after a set time, when the derivative of the force was negative, i.e. when the force in the belt started to reduce. The belt property between locking and belt offloading was approximated as linear stiffness (parameter two) (see Fig. A1). The two parameters were varied separately.

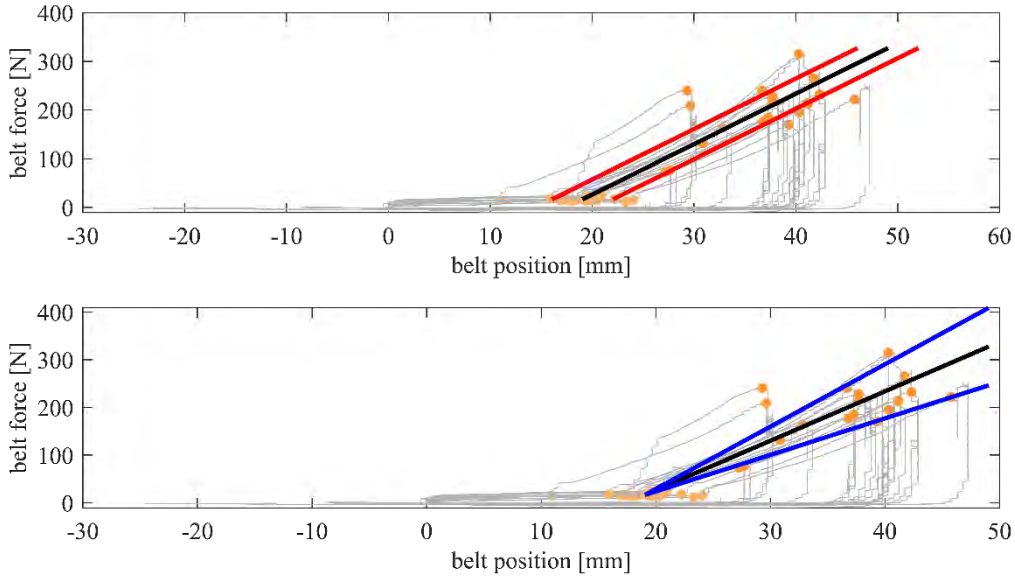

Fig. A1. Belt force-displacement curves. The light orange dots indicate belt locking, and the dark orange circles indicate maximum force in the locked range. The black lines show the average linearly approximated belt force-displacement after locking, at average lock force-displacement. In the top figure, the displacement at locking parameter is shown, with ±1 SD in red. In the bottom figure, the belt slope parameter is shown, with ±1 SD in blue.

Vehicle acceleration shape and change in velocity

The acceleration pulses of all braking events from [27] were analysed with principal component analysis (PCA) [51-53] to identify the most important variability. Prior to PCA, accelerations were normalised with the velocity change (dv), based on integrated acceleration. Velocity change and the shape of acceleration (using the first principal component, PC 1) was varied in the boundary condition sensitivity study, (Fig. A2).

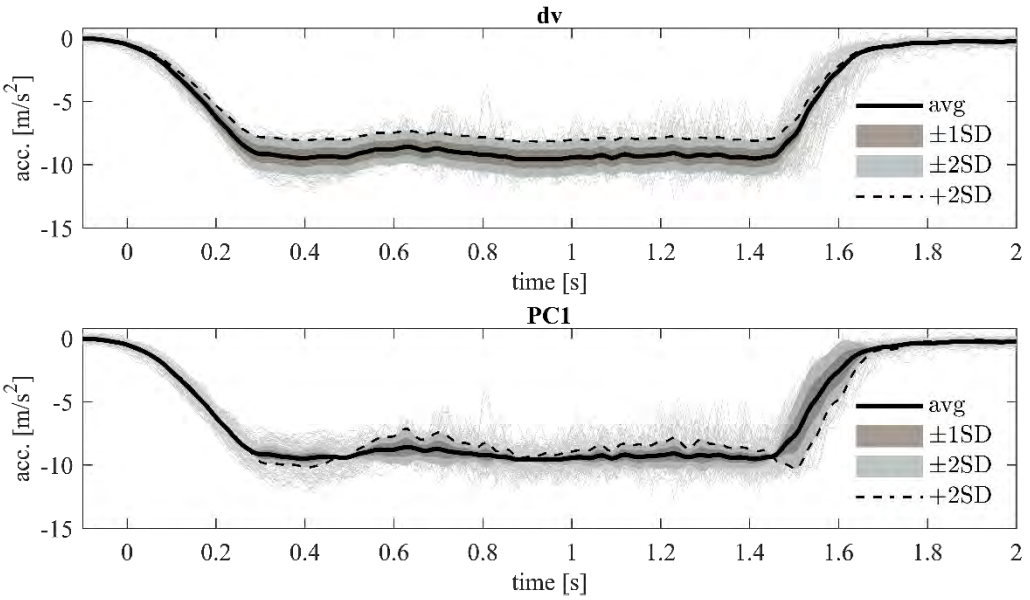

Fig. A2. Acceleration: grey curves from tests [27], average acceleration in black. In the upper figure, average ±1 SD (filled brown) and ±2 SD (filled grey) for velocity change is highlighted. In the lower figure, average ±1 SD (filled brown) and ±2 SD (filled grey) for shape (PC1) is highlighted. In both figures, dashed line shows +2 SD. (Note: since the velocity change was negative, +2 SD decreases the magnitude of velocity change.)

Seat and D-ring positions

In the experiments, the seat could move 220 mm in the longitudinal direction, and the seat was moved longitudinally so the volunteers had their feet on the footrest. The seat longitudinal position for each volunteer was not recorded. In the sensitivity study, the seat longitudinal position was assumed to be uniformly distributed,

with the nominal position in the mid-travel position. Instead of moving the seat as in the volunteer tests, the D-ring was moved in the longitudinal direction in the simulation study (blue movements in Fig. A3).

In the experiment the D-ring was kept at the mid-position, and the seat vertical position was kept constant. Since the volunteers had different seated heights, the shoulder to D-ring distance varied based on each volunteer's seated height. This variation was included in the sensitivity study by moving the D-Ring and the B-pillar structure in the vertical direction (i.e. not using the D-ring sliding mechanism). The distribution was assumed uniform between the maximum (990 mm) and minimum (894 mm) seated heights among the male volunteers, with the nominal position from D-ring relative seat position used in experiments assumed to correspond to mid-point between maximum and minimum seated heights (red movements in Fig. A3).

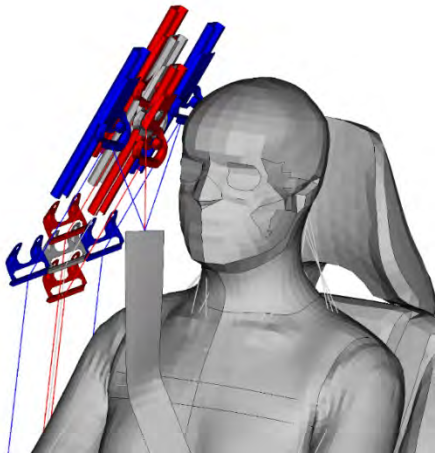

Fig. A3. D-ring position variations, with nominal in grey, forward-rearward variations in blue, and upward-downward variations in red.

Friction coefficient

The friction between the HBM and the seat was also included in the boundary condition sensitivity study. In the nominal model, a coefficient of 0.3 was used for both static and dynamic friction, similar to previous simulations of the braking manoeuvre. In the parameter variation, the distribution was assumed to be uniform between 0.1 and 0.5, with upper and lower limit based on values from a study by [39]. However, compared to that study, the lower limit was decreased from 0.15 to 0.1 to get a symmetric distribution around the nominal value.

Arm constraints

The arms were constrained to the thighs using constant force cables. The nominal force in the cables was initially tuned to 10 N, to prevent the arms from introducing excessive inertia load in the upper torso, without over-constraining the torso to the thighs. To further investigate the sensitivity of the cable force, the force was varied in the boundary condition sensitivity study. A uniform distribution between 0 N and 20 N was used.

Appendix III - Latin hypercube sampled parameter variations used in the study on synthetic experimental series

TABLE AI
LATIN HYPERCUBE SAMPLED PARAMETER VARIATIONS

BeltSlope [N/mm]	PCSA [-]	Seatpos [mm]	SpinePC1 [-]	SpinePC2 [-]	Dv [m/s]
6,89	0,98	-95,35	11,27	9,21	-12,66
12,22	1,08	-53,33	-36,31	-11,21	-13,31
11,72	1,13	11,35	-88,76	32,24	-12,54
5,74	1,24	92,64	46,62	38,77	-11,78
10,81	0,97	48,58	97,83	-7,75	-14,02
7,46	1,04	-82,75	7,27	-23,44	-12,65

10,41	0,86	84,71	-17,87	-44,14	-12,32
8,39	1,39	60,82	133,96	-29,39	-12,31
12,91	0,68	75,53	-47,47	64,02	-12,12
13,31	0,75	-104,34	25,26	24,58	-13,68
10,35	0,91	-66,72	-8,77	-74,00	-13,12
12,07	0,89	22,39	52,13	-18,66	-11,54
9,10	0,82	35,97	63,37	1,55	-11,93
14,68	0,95	-21,38	27,91	-37,50	-11,15
11,17	1,01	-34,92	-70,31	-3,88	-10,91
9,77	1,07	-14,78	-125,95	-13,27	-14,10
8,69	1,28	-76,21	-49,97	44,27	-12,81
7,92	1,15	44,86	84,32	4,68	-11,75
15,61	1,18	-0,89	-26,30	15,95	-13,43
9,64	0,80	-45,05	-115,97	18,51	-12,98